

## STUDY ON DEFORMATION CAPACITY OF REINFORCED CONCRETE CORE WALLS AFTER FLEXURAL YIELDING

T. Hatakenaka<sup>1</sup> and T. Nakachi<sup>2</sup>

<sup>1</sup> *Ishiguro Corporation, Fukui, Japan*

<sup>2</sup> *Professor, Dept. of Architecture and Civil Engineering, Architecture Major,  
 Fukui University of Technology, Fukui, Japan  
 Email: nakachi@fukui-ut.ac.jp*

### ABSTRACT:

In a core wall system high-rise building, the center core of which consists of four L-shaped core walls, the axial load of the core wall is very high when a diagonal seismic force occurs. In particular, the corner and the area near the corner of an L-shaped core wall are subjected to high compressive stress, so it is considered to be effective to reinforce these areas for improving the deformation capacity of core walls. In this study, central compression tests and eccentric compression tests were conducted on square and rectangular section columns which simulated the corner and the area near the corner of the L-shaped core walls. The results of these compression tests were analyzed using the three-dimensional nonlinear finite element method (FEM), and the deformation capacity of core walls was examined. The tests and analyses showed that increasing the confining area of concrete, the amount of confining steel and so on were shown to be effective for improving the deformation capacity of core walls.

**KEYWORDS:** core wall, deformation capacity, compression test, confining steel, FEM analysis

### 1. INTRODUCTION

In order to examine the deformation capacity of core walls, central compression tests and eccentric compression tests were conducted on square and rectangular section columns which simulated the corner and the area near the corner of L-shaped core walls. The parameters of the central compression tests were the amount of confining steel and the compressive strength of concrete. The compressive strength of concrete used was 42 – 80 N/mm<sup>2</sup>. High-strength reinforcement bars were used for the confining steel. The parameters of the eccentric compression tests were the area of concrete confinement, the amount of confining steel, and the type of concrete confinement. The type of concrete confinement was tie bar and closed reinforcement. The compressive strength of concrete in the eccentric compression tests was 60 N/mm<sup>2</sup>. The results of these compression tests were analyzed using three-dimensional nonlinear FEM, and the deformation capacity of the core walls was examined.

### 2. CENTRAL COMPRESSION TESTS

#### 2.1 Test Specimen

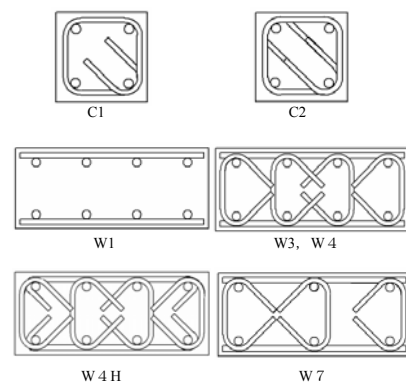


Fig. 1 Test specimens

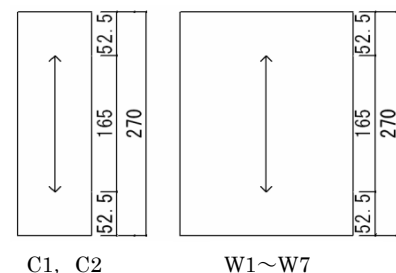


Fig. 2 Measuring system

The configuration and arrangement of reinforcement in the specimens are shown in Fig. 1. The characteristics of the specimens are listed in Table 1. The physical properties of the concrete and reinforcement are listed in Table 2 and Table 3, respectively. The arrangement of reinforcement was identical with square section Specimens C0 – C2, which simulated the corner of wall columns, and rectangular section Specimens W0, W1, W4, and W7, which simulated the panel of wall columns of Fc 60 series tested previously<sup>1)</sup>. The specimens of this series were different from that of the Fc 60 series in the strength of concrete; the strength of concrete in this series is 42 N/mm<sup>2</sup> and 80 N/mm<sup>2</sup>. As the specimen of the Fc 42 series, Specimen W3 was added.

The vertical pitch of the horizontal reinforcement (D6) in each specimen was 55 mm. The vertical pitch of confining steel (U5.1) was 27.5 mm in Specimens W4, W4H, and W7, and 55 mm in Specimens C1, C2, and W3. The horizontal pitch of the longitudinal reinforcement (D10) was 55 mm except for 82.5 mm of Specimen W7. Normal-strength reinforcement was used for the confining steel of Specimen C1 and high-strength reinforcement was added to the normal-strength reinforcement for Specimen C2. Specimen W4H was hooked at the end of the horizontal reinforcement for Specimen W4.

## 2.2 Test Procedure

Figure 2 shows the measuring system. Test specimens were subjected to monotonic uni-axial compression. Axial strain was measured by transducer. The measuring length was 165 mm. Strain gages were attached to the confining steel, the horizontal reinforcement and the longitudinal reinforcement.

## 2.3 Test Results

Table 4 shows the test results. In the square section Specimens 42C0, 42C1 and 42C2, the maximum stress and the strain at the maximum stress increased corresponding to the increment of confining steel. These values of Specimen C2, which had both of the normal-strength reinforcement and the high-strength reinforcement, were particularly large. In rectangular section specimens of the Fc 42 series, the strain at the maximum stress of Specimen 42W4H, which was hooked at the end of the

Table 1 Test specimens

Specimen	Fc (N/mm <sup>2</sup> )	Configuration at cross section (mm)	Type of confining steel	Vertical pitch of confining steel (mm)	Horizontal pitch of confining steel (mm)
42C0	42	90×90	—	—	—
42C1	42	90×90	hoop	55	55
42C2	42	90×90	hoop	55	55
42W0	42	90×210	—	—	—
42W1	42	90×210	—	—	55
42W3	42	90×210	tie	55	55
42W4	42	90×210	tie	27.5	55
42W4H	42	90×210	tie	27.5	55
42W7	42	90×210	tie	27.5	82.5
60C0	60	90×90	—	—	—
60C1	60	90×90	hoop	55	55
60C2	60	90×90	hoop	55	55
60W0	60	90×210	—	—	—
60W1	60	90×210	—	—	55
60W4	60	90×210	tie	27.5	55
60W7	60	90×210	tie	27.5	82.5
80C0	80	90×90	—	—	—
80C1	80	90×90	hoop	55	55
80C2	80	90×90	hoop	55	55
80W0	80	90×210	—	—	—
80W1	80	90×210	—	—	55
80W4	80	90×210	tie	27.5	55
80W4H	80	90×210	tie	27.5	55
80W7	80	90×210	tie	27.5	82.5

Table 2 Physical properties of concrete

Specimen	Compressive Strength $\sigma_B$ (N/mm <sup>2</sup> )	Young's Modulus * ( $\times 10^4$ N/mm <sup>2</sup> )	Split Strength (N/mm <sup>2</sup> )
Fc42series	45.9	2.65	5.14
Fc60series	62.8	3.49	3.61
Fc80series	80.7	3.54	5.93

\*Secant Modulus at one-third of  $\sigma_B$

Table 3 Physical properties of steel

Bar Size	Yield Strength (N/mm <sup>2</sup> )	Maximum Strength (N/mm <sup>2</sup> )	Young's Modulus ( $\times 10^5$ N/mm <sup>2</sup> )	Elongation (%)
D6	407	554	2.28	22.5
D10	387	586	2.05	24.8
U5.1	1446	1456	2.03	11.3

Yield strength of D6, U5.1: 0.002 off set

Table 4 Test results

Specimen	Maximum Load (kN)	Maximum Stress (N/mm <sup>2</sup> )	Strain at Max. Load (%)
42C0	301.9	37.3	0.24
42C1	389.4	48.1	0.48
42C2	417.5	51.5	0.88
42W0	644.2	34.1	0.16
42W1	876.8	46.4	0.16
42W3	819.3	43.4	0.29
42W4	867.0	45.9	0.91
42W4H	1028.4	54.4	1.40
42W7	864.4	45.7	0.16
80C0	480.9	59.4	0.21
80C1	615.5	76.4	0.30
80C2	616.1	76.1	0.82
80W0	1166.9	61.7	0.48
80W1	1468.1	77.7	0.31
80W4	1343.3	71.1	0.47
80W4H	1586.4	83.9	1.14
80W7	1374.0	72.7	0.40

horizontal reinforcement, was particularly large. The results of the  $F_c$  80 N/mm<sup>2</sup> series were approximately similar to those of the  $F_c$  42 N/mm<sup>2</sup> series.

Figure 3 shows the relationship between specimen axial compressive stress  $\sigma$  ( $= N/A$ ,  $N$ : axial load,  $A$ : section area) and axial strain. Figure 3(a) shows the results of Specimens 42C2, 60C2, and 80C2. Figure 3(b) shows the results of Specimens 42W4, 60W4, and 80W4. In the figures, the drop in stress after the maximum was larger corresponding to the increment of compressive strength of concrete. Figure 3(c) shows the results of Specimen 42W4H which was hooked at the end of the horizontal reinforcement, Specimen 42W4 without hook, Specimen 42W3 which had twice the vertical pitch compared with the other specimens, and Specimen 42W7 of which the horizontal pitch of longitudinal reinforcement was 82.5 mm compared with 55 mm of the other specimens. The maximum stress, the strain at the maximum stress, and the stress after the maximum stress of Specimen 42W4H with hook were larger than those of Specimen 42W4H without hook. The reason for these results is considered to be that the specimen with hook had a confinement effect of concrete by the hook. The confinement effect of Specimens 42W3 and 42W7, especially that of 42W7, is considered to be smaller than that of 42W4. The reason for these results is considered to be the increment of failure area and the decrement of volume ratio of confining steel by the increment of horizontal pitch of the longitudinal reinforcement. Therefore, regarding the pitch of confining steel, not only the vertical pitch proposed previously but also the horizontal pitch should be taken into account when calculating the confinement effect of concrete. Figure 3(d) shows the results of Specimen 80W4H with hook, Specimen 80W4, and Specimen 80W7 of which the horizontal pitch of longitudinal reinforcement was 82.5 mm. The results of these specimens were approximately similar to those of the  $F_c$  42 N/mm<sup>2</sup> series shown in Fig. 3(c).

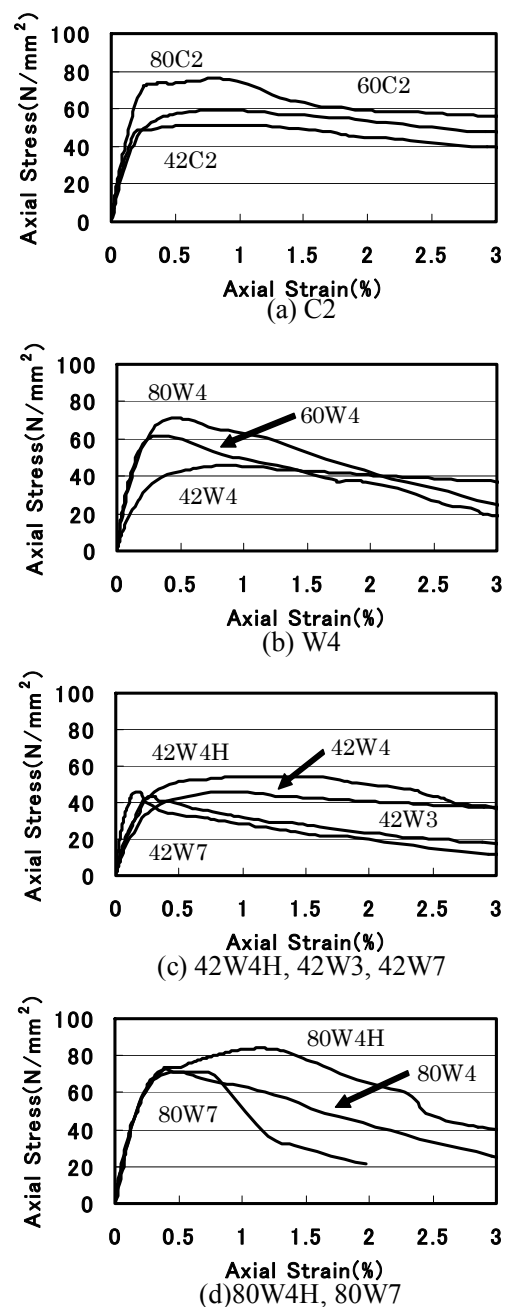


Fig. 3 Axial stress versus axial strain curves

Figure 4 shows the relationship between the strain of the reinforcement and the axial strain of Specimens 42W4 and 42W4H. Gages 1 and 3 were attached at the center level of the specimens, while gages 2 and 4 were attached at one pitch above the center level. Gages 1 and 2 were attached to the high-strength confining steel, and gages 3 and 4 were attached to the normal-strength horizontal reinforcement. Figure 4(a) shows the results of 42W4 without hook. The strain of gages 3 and 4 on the horizontal reinforcement without hook was approximately  $0\mu$  at the axial strain of 0.5% whereas

the strain of gages 1 and 2 on the high-strength confining steel was approximately  $2000\mu$  till around the axial strain of 3%. It is considered that the confinement effect of the horizontal reinforcement of Specimen 42W4 hardly influenced the increment of the maximum stress because the maximum stress of Specimen 42W4 occurred after the axial strain of 0.5%. Figure 4(b) shows the results of 42W4H with hook. The strain of gages 1 and 2 on confining steel was approximately the same as the results of 42W4 shown in Fig. 4(a). On the other hand, the strain of gages 3 and 4 on the horizontal reinforcement with hook continued to increase after the axial strain of 0.5%, different from Specimen 42W4. In particular, the strain of gage 4 increased up to  $10000\mu$  at around the axial strain of 2.5%. It is considered that the confinement effect occurred in the longitudinal direction of section by hook and the compressive ductility of Specimen 42W4H was therefore larger than that of Specimen 42W4 shown in Fig. 3(c). The relationship between the strain of the reinforcement and the axial strain in the Fc 80 N/mm<sup>2</sup> series was the same as that of the Fc 42 N/mm<sup>2</sup> series. As above, the hook at the end of the horizontal reinforcement is remarkably effective for improving the confinement effect in the longitudinal direction. That is, the hook which is arranged to anchor the horizontal reinforcement also effectively improves the compressive ductility of the edge area concrete of which the boundary condition is approximately the same as in these compression tests.

### 3. ECCENTRIC COMPRESSION TESTS

#### 3.1 Test Specimen

The configuration and arrangement of reinforcement in the specimens are shown in Fig. 5. The characteristics of the specimens are listed in Table 5. The physical properties of the concrete and reinforcement are listed in Table 6 and Table 7, respectively. The configuration of the specimens was identical with that of the central compression tests. The specified design concrete strength was 60 N/mm<sup>2</sup>. Seven arrangements of specimens were tested: Specimens WE1 – WE7. The vertical pitch of the horizontal reinforcement (D6) and the horizontal pitch of the longitudinal reinforcement (D10) were both 55 mm. The vertical pitch of confining steel was 55 mm except for Specimen WE5 of which the vertical pitch was 27.5 mm.

#### 3.2 Test Procedure

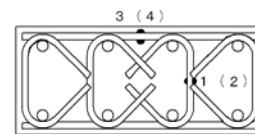
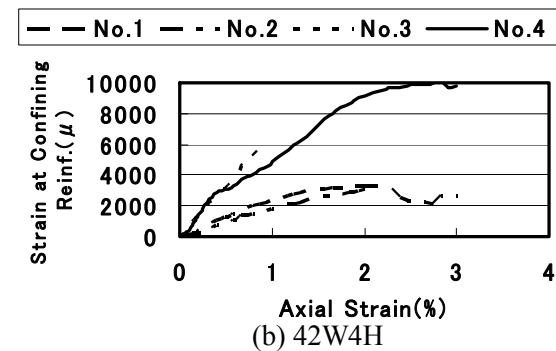
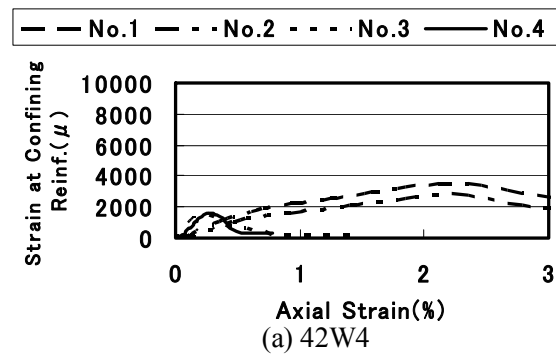


Fig. 4 Strain of reinf. versus axial strain curves

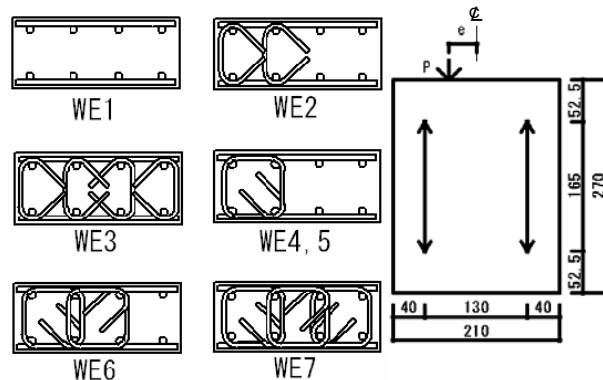


Fig. 5 Test specimens Fig. 6 Measuring system

Figure 6 shows the measuring system. Test specimens were subjected to monotonic uni-axial compression with a distance of eccentricity  $e$  from the center. The pin support was set at the top of the specimens. Axial strain was measured by transducer. Measuring length was 165 mm. Strain gages were attached to the confining steel, the horizontal reinforcement and the longitudinal reinforcement. The eccentricity was 35 mm and 17.5 mm for each of Specimens WE1 – WE7. A suffix of -06 and -12 was added to the specimen name in the case of eccentricity  $e$  of 35 mm ( $e = D/6$ ,  $D = 210$  mm) and 17.5 mm ( $e = D/12$ ), respectively. Two kinds of eccentricities were fixed for the two kinds of axial stress level because the compressive area of the core walls at the bottom depended on the level of axial stress. The eccentricity of 35 mm is assumed to be at a lower axial stress level than that of 17.5 mm.

### 3.3 Test Results

Table 8 shows the test results. In the table, the maximum moment is the product of the maximum load and eccentricity. The curvature was found by dividing the difference of strains measured by the two transducers shown in Fig. 6 by the distance between the two transducers.

#### 3.3.1 Relationship between moment and curvature at an eccentricity of 35 mm

Figures 7(a) and (b) show the relationship between moment and curvature at an eccentricity of 35 mm. Figure 7(a) shows the results of Specimen WE2-06 which was confined at the edge area by tie bars, Specimen WE3-06 which was confined over the entire area by tie bars, and Specimen WE1-06 without

confining steel. The maximum moment, the curvature at the maximum moment, and the moment after the maximum moment of specimens with confining steel were larger than those of specimens without confining steel. The difference of the relationship between moment and curvature with the difference in confining area was smaller than that of specimens confined with closed reinforcement as described next. Figure 7(b) shows the results of Specimen WE4-06 which was confined at the edge area by closed reinforcement, Specimen WE7-06 which was confined over the entire area by closed reinforcement, Specimen WE6-06 which was confined at the intermediate area of Specimen WE4-06 and WE7-06, and Specimen WE5-06 which had twice the amount of confining steel as Specimen WE4-06.

Table 5 Test specimens

Specimen	$F_c$ (N/mm <sup>2</sup> )	Segment at configuration (mm)	Type of confining steel	Vertical pitch of confining steel (mm)	Eccentricity (mm)	
WE1-06	60	90	—	—	35	
WE2-06			tie	55	35	
WE3-06			tie	55	35	
WE4-06			hoop	55	35	
WE5-06			hoop	27.5	35	
WE6-06			hoop	55	35	
WE7-06			hoop	55	35	
WE1-12		210	—	—	—	17.5
WE2-12			tie	55	17.5	
WE3-12			tie	55	17.5	
WE4-12			hoop	55	17.5	
WE5-12			hoop	27.5	17.5	
WE6-12			hoop	55	17.5	
WE7-12			hoop	55	17.5	

Table 6 Physical properties of concrete

Compressive Strength $\sigma_B$ (N/mm <sup>2</sup> )	Young's Modulus * ( $\times 10^4$ N/mm <sup>2</sup> )	Split Strength (N/mm <sup>2</sup> )
65.7	2.96	2.82

\*Secant Modulus at one-third of  $\sigma_B$

Table 7 Physical properties of steel

Bar Size	Yield Strength (N/mm <sup>2</sup> )	Maximum Strength (N/mm <sup>2</sup> )	Young's Modulus ( $\times 10^5$ N/mm <sup>2</sup> )	Elongation (%)
D6	378	563	1.94	24.3
D10	380	532	1.89	25.7
U5.1	1467	1492	2.07	11.5

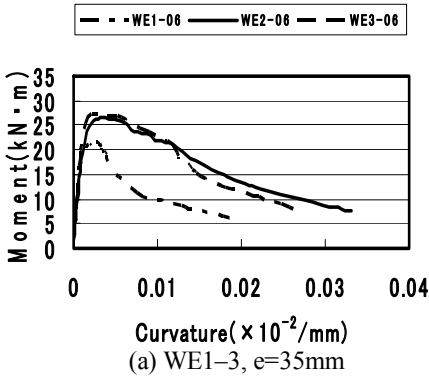
Yield strength of D6, U5.1: 0.002 off set

Table 8 Test results

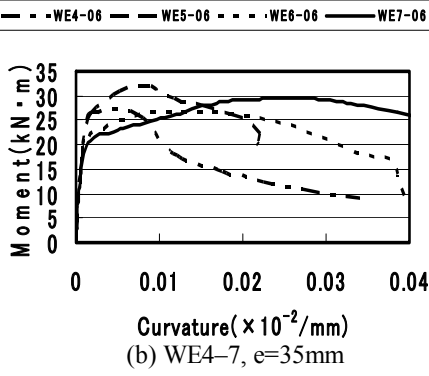
Specimen	Maximum moment (kN·m)	Curvature at Max. moment ( $\times 10^{-2}$ /mm)
WE1-06	21.5	0.0027
WE2-06	26.5	0.0035
WE3-06	27.4	0.0029
WE4-06	27.4	0.0047
WE5-06	32.2	0.0081
WE6-06	26.8	0.0137
WE7-06	29.5	0.0267
WE1-12	15.8	0.0006
WE2-12	14.7	0.0024
WE3-12	13.5	0.0017
WE4-12	16.7	0.0044
WE5-12	16.4	0.0039
WE6-12	16.0	0.0092
WE7-12	17.3	0.0147



In comparison between Specimens WE4-06, WE6-06, and WE7-06 which had the same vertical pitch of confining steel but different confinement areas, the maximum moment of Specimen WE7-06 confined over the entire area was largest among all the specimens. The curvature at the maximum moment was larger corresponding to the larger confinement area. The drop in the moment after the maximum moment was smaller corresponding to the larger confinement area. The difference of the relationship between moment and curvature is remarkable in comparison with the specimens with tie bars shown in Fig. 7(a).



In comparison between Specimens WE4-06 and WE5-06 which had different amounts of confining steel, the maximum moment and the curvature at the maximum moment were larger corresponding to the larger amount of confining steel. However, the curvature of Specimen WE5-06 with more confining steel began to decrease as the moment declined after reaching the maximum, whereas the curvature of Specimen WE4-06 continued to increase till the final stage of loading. The reason for the decrease of curvature is considered as follows. Specimen WE5-06 had twice the amount of confining steel as Specimen WE4-06. Therefore, the confined concrete withstood the large compressive stress till the large axial strain and the axial strain of the adjoining area without confinement increased. As a result, the stress of the area without confinement decreased instantly. In some of the lateral loading tests of core walls conducted previously, crumbling of the concrete at the inside area without confinement adjoining the edge area confined by confining steel was reported to cause the final decrease of the lateral load of specimens. The results of Specimen WE5-06 are considered to correspond to such results of lateral loading tests. Therefore, the core wall confined at only the furthest edge area is considered to be at risk of an instant decrease of lateral load.



3.3.2 The relationship between moment and curvature at an eccentricity of 17.5 mm

Figures 7(c) and 7(d) show the relationship between moment and curvature at an eccentricity of 17.5 mm. Figure 7(c) shows the results of Specimen WE2-12 which was confined at the edge area by tie bars, Specimen WE3-12 which was confined over the entire area by tie bars, and Specimen WE1-12 without confining steel. The maximum moment of Specimen WE1-12 without confining steel was a little larger than that of specimens with confining steel, and its moment decreased instantly after the maximum moment. The difference of the relationship between moment and curvature due to the difference of the

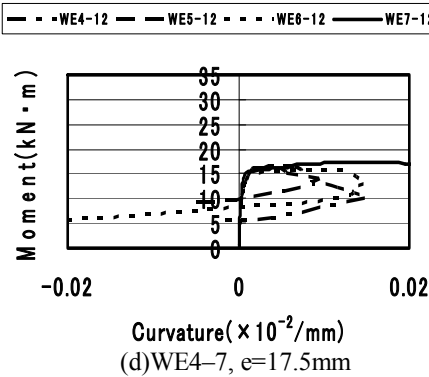
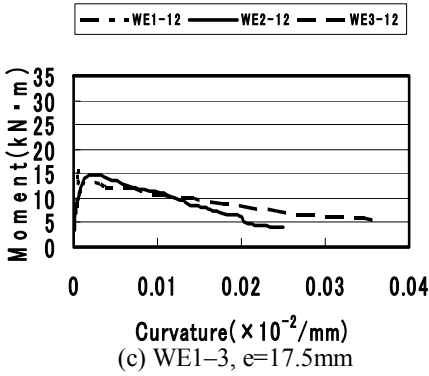


Fig. 7 Moment versus curvature curves

confinement area was smaller than that of specimens confined with closed reinforcement mentioned next.

Figure 7(d) shows the results of Specimen WE4-12 which was confined at the edge area by closed reinforcement, Specimen WE7-12 which was confined over the entire area by closed reinforcement, Specimen WE6-12 which was confined at the intermediate area of Specimen WE4-06 and WE7-06, and Specimen WE5-12 which had twice the amount of confining steel as Specimen WE4-06. The curvature of Specimen WE4-12 and WE6-12 began to decrease as the moment declined after reaching the maximum, whereas the curvature of Specimen WE7-12 which was confined over the entire area continued to increase till the final stage of loading. The reason for the results is considered that the loading point was near to the center of specimens and therefore the compressive stress at the area without confining steel was larger than that of specimens with an eccentricity of 35 mm. In comparison between Specimens WE4-12 and WE5-12 which had different amounts of confining steel, both specimens began to decrease when the moment started to decline after reaching the maximum. The reason for the results is also considered to be the large stress at the area without confining steel. The specimens with an eccentricity of 17.5 mm are assumed to be the core walls at larger axial load than that with an eccentricity of 35 mm. Therefore, the compressive stress at the area without confining steel of the core walls with large axial load is large, and a larger area with confining steel is needed than for core walls with small axial load.

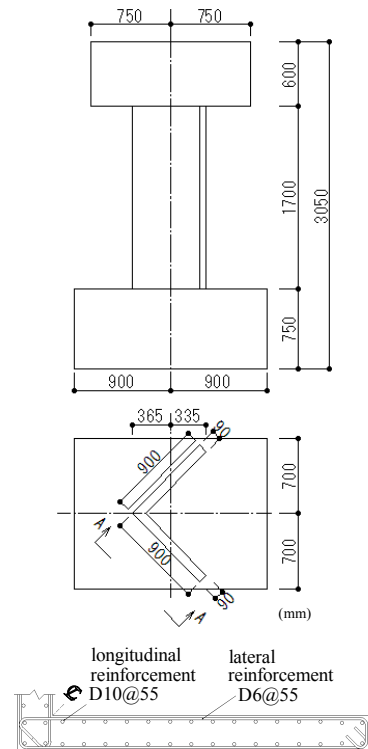


Fig. 8 Analyzed specimens

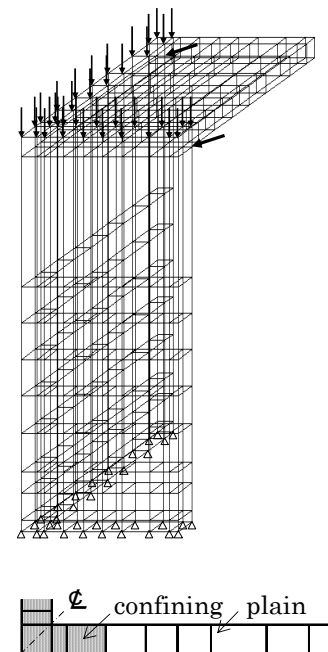


Fig. 9 Analytical models

## 4. FEM ANALYSIS OF CORE WALLS

### 4.1 Analytical Models and Analytical Procedure

Figure 8 shows the analyzed specimens of lateral loading tests of core walls<sup>1)</sup>. The specimens were one-eighth-scale and represented the core walls of the lower three stories of a high-rise building. The specimens had a shear span ratio of 2.5. The analytical models of specimens are shown in Fig. 9. The analysis was done using three-dimensional nonlinear FEM. Four models were analyzed. Model 1 was a standard model of which the confinement area corresponded to Specimen 42W4 of the compression tests. The axial stress of Model 1 was 40% of the compressive strength of concrete. Models 2 and 3 corresponded to Specimen 80W4 and 42W3, respectively. Model 4 corresponded to Specimen 42W4 and its axial stress was 50% of the compressive strength of concrete. Concrete was represented by 8-node isoparametric solid elements. The physical properties of concrete and the reinforcement in the central compression tests were used for the analytical model. The failure curve of bi-axial compression was represented by Omuma's model<sup>2)</sup>. The compressive descending stress-strain relationships were linear. The concrete confining effect was represented by the results of the central compression tests mentioned above. The reinforcement was assumed to be a linear element, and the stress-strain relationships of the reinforcement were assumed to be bilinear. The analytical models were subjected to monotonic loading. After constant axial loading, the model was loaded laterally.

## 4.2 Analytical Results

Figure 10 shows the load-deflection curves of Models 1 to 4. The drop in load after the maximum load of Models 2, 3, and 4 was larger than that of Model 1. That is, the deformation capacity of a model was smaller with larger compressive strength of concrete, smaller amount of confining steel, and larger axial stress. These analytical results show the effects of the compressive strength of concrete, the amount of confining steel, and the axial stress on the deformation capacity of core walls. Regarding the axial stress, the ratio of confinement area for the compressive area was considered to be smaller corresponding to the increment of axial stress.

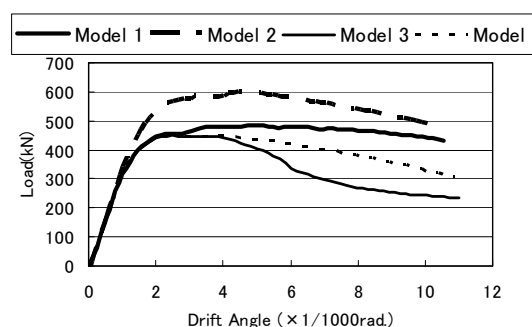


Fig. 10 Load-deflection curves

## 5. CONCLUSIONS

Central compression tests and eccentric compression tests were conducted on square and rectangular section columns which simulated the corner and the area near the corner of L-shaped core walls. The results of these compression tests were analyzed using three-dimensional nonlinear FEM. The major findings were as follows:

- (1) The drop in stress after the maximum of rectangular section specimens was larger with higher compressive strength of concrete. The results were identical to those of compression tests using square section specimens conducted previously.
- (2) The confinement effect is considered to decrease with larger horizontal pitch of confining steel by the increment of failure area and decrement of volume ratio of confining steel.
- (3) The hooks, which are arranged for the anchor of horizontal reinforcement, are also considered to be effective for improving the compressive ductility of edge area concrete.
- (4) The compressive ductility of specimens with closed confining steel was larger corresponding to the larger confinement area.
- (5) Some of the specimens with a large amount of confining steel at the edge area crumbled at the area without confinement before crumbling at the area with confinement.
- (6) The specimens with an eccentricity of 17.5 mm showed a larger decrease of curvature than that with an eccentricity of 35 mm.
- (7) FEM analysis showed that the deformation capacity of the model was smaller with larger compressive strength of concrete, smaller amount of confining steel, and larger axial stress.

## ACKNOWLEDGMENTS

This work was supported by the FUT Research Promotion Fund. The authors are grateful for the support.

## REFERENCES

- 1) Nakachi, T., Toda, T. and Tabata, K. (1996). Experimental Study on Deformation Capacity of Reinforced Concrete Core Walls after Flexural Yielding. *Proceedings of Eleventh World Conference on Earthquake Engineering*, Paper No. 1714.
- 2) JSCE. (1981). New Civil Engineering Series 29, Gihodo Shuppan.